Electrical spectroscopy of GaAs with intrinsic illumination: The optical recovery of *EL2*

K. Khachaturyan, E. R. Weber, and J. Horigan
Department of Materials Science and Mineral Engineering, University of California, Berkeley, California 94720
and Materials Science Division, Lawrence Berkeley Laboratory, Berkeley, California 94720
(Received 6 September 1991)

We extend the technique of photoconductance and photocapacitance characterization of semiconductors to excitation energies above the band gap. Intrinsic illumination was found to cause highly efficient recovery of *EL2* in semi-insulating GaAs from the metastable state at 4 K and to quench extrinsic photoconductance. The results indicate that this optical recovery is a recombination-enhanced defect reaction, triggered by hot-electron capture into a resonant acceptor level of the metastable state of *EL2* with a capture barrier of 0.07 eV.

I. INTRODUCTION

The dominant defect in undoped semi-insulating GaAs is the so-called *EL2* defect, which is related to an arsenic antisite defect.[1] The characteristic optical absorption of *EL2* can be quenched at low temperatures by illumination, which is explained by a transition of *EL2* into a metastable, lattice-relaxed state *EL2**. *EL2* can be recovered from its metastable state thermally with an activation energy of 0.34 eV, but this activation barrier is reduced to 0.107 eV in the presence of electrons, which are provided either through doping[1] or via photoexcitation.[2] This possibility of optically assisted thermal recovery requiring temperatures above 60 K is frequently confused with the true optical recovery. It was not clear whether optical excitation alone can induce the $EL2^{*} \Longrightarrow EL2^{0}$ transformation (or *EL2* recovery) even at liquid-helium temperature. In the present work, the study of the *EL2* optical recovery is extended to above-band-gap illumination. While Tajima[3] and Fischer[4] observed low-efficiency *EL2* recovery (three orders of magnitude smaller than the photoquenching efficiency) by 0.94- and 1.46-eV illumination, respectively, other authors[2] claim that optical recovery at such low temperatures is impossible. Recently, Baj and Dreszer[5–7] observed efficient optical recovery of *EL2* at 4 K at hydrostatic pressure $p > 0.3$ GPa. They have shown[7] that the key role in *EL2* optical recovery is played by the acceptor level $(EL2^{*})^{-/0}$, resonant with the conduction band under ambient pressure but driven into the band gap at $p > 0.3$ GPa, and populated by below-band-gap illumination. According to their model,[7] the energy needed for the transformation of *EL2* from the metastable to the ground state is supplied by electron-hole recombination at the acceptor level $(EL2^{*})^{-/0}$. Observation of $EL2^{*} \Longrightarrow EL2^{0}$ conversion[8] by electron pulse irradiation at 10 K supported that conclusion.

The study of the optical recovery of *EL2* from the metastable state was extended to above-band-gap illumination. Extension of photocapacitance and photoconductance measurements to excitation energies above the band gap was made possible by the use of microfabricated interdigitated capacitor structures.

II. EXPERIMENT

In this work, a spectroscopic method which permits optical characterization of a defect energy level resonant in the conduction or the valence band is developed. For this purpose, excitation with photon energy above the band gap should be used. This is impossible in a conventional optical absorption or a photoconductance experiment, because of the very high absorption coefficient ($\sim 10^{4}$ cm^{-1}) of above-band-gap light in direct-band-gap semiconductors. The absorption of the above-band-gap light due to band-to-band excitation is many orders of magnitude greater than by defects, making special techniques necessary. The penetration depth of the light is about the inverse of the optical-absorption coefficient; for the case of GaAs, the penetration depth of above-band-gap illumination is thus less than 1 μm.

The sampling depth in a photoconductivity experiment is of the order of the distance between the electrodes. Usually, the distance between electrodes is equal to the sample thickness, typically a few millimeters. Therefore, in a conventional photoconductivity experiment the sampling depth is also a few millimeters, so that photoconductivity measurements are generally dominated by properties of bulk samples. A conventional photoconductivity experiment would not be sensitive to a defect reaction, occurring only within the micrometer thick layer near the surface, e.g., after excitation by above-band-gap illumination. In this work, the photoconductivity measurement is modified into a surface sensitive technique. For that purpose, electrodes of opposite polarity should be spaced only a few micrometers apart. In this work, 160 pairs of $\lambda/4$-thick, 70λ-wide electrodes of opposite polarity spaced by $\lambda/4$ form an interdigitated capacitor [Fig. 1(a)]. The periodic surface charge distribution [Fig. 1(b)] on the electrodes of the interdigitated capacitor produces an electric field exponentially decaying away from the surface as $\exp(-2\pi z/\lambda)$ for $z \gg \lambda/6\pi$ (see the Appendix). Note that the exponentially decaying field is due to the spatial periodicity of the electrodes. Since the photoconductance is a convolution of the photoconductivity with the electric field, the main contribution to the photoconductance arises for this case from the top

$\lambda/2\pi = 3.2$ μm thick layer near the surface. This sampling depth is comparable to the penetration depth of approximately 1 μm of the light just above the band gap.[9]

For dc photoconductance measurements, 800 Å Au-Ge metallization, which formed Ohmic contacts after being annealed at 450 °C, was deposited, and the two-terminal resistance was measured with an ohm meter. However, the contacts on semi-insulating GaAs cannot be made perfectly Ohmic. Therefore, a more accurate photoconductance value can be obtained, it the measurement is done at a high frequency. At high frequencies, the series capacitative impedance of even a rectifying contact is quite low. As a result, for high-frequency photoconductance measurements, the properties of the contacts (Ohmic vs rectifying) are not important. The high-frequency conductance and capacitance were simultaneously measured with a HP4280A capacitance meter at 1 MHz. Rectifying contacts were formed by evaporation of 600 Å of aluminum. In this work, dc and rf measurement produced very similar results, but the precision of the ac measurements was better.

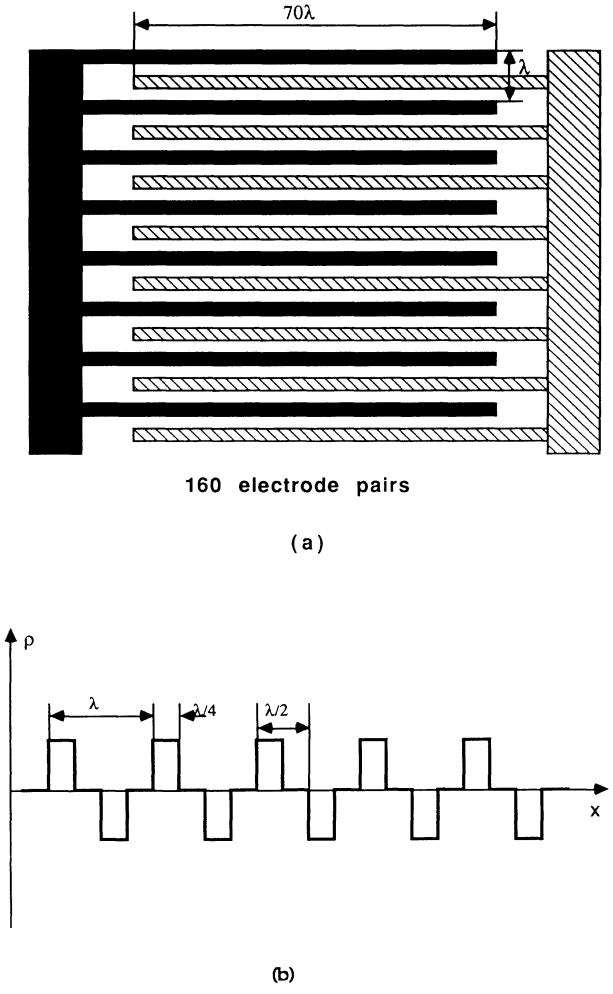

FIG. 1. (a) A periodic array of electrodes of alternating polarity, used for the photoconductance and photocapacitance measurements. (b) Surface charge-density distribution of the structure in 1(a).

The same problem of being unable to extend the measurements to above-band-gap excitation energies is encountered also in conventional photocapacitance experiments. In the standard photocapacitance technique, a metal dot is deposited on the surface of a semiconductor, forming a Schottky barrier. However, since the metal forming the Schottky barrier is not transparent, in a conventional photocapacitance experiment the sample is illuminated from the back, unmetallized side. This again makes it impossible to measure photocapacitance due to above-band-gap illumination, which cannot penetrate from the back to the front side of the sample.

This major difficulty can again be circumvented, in the same way as in the case of photoconductivity measurements, with the use of a periodic structure of interdigital electrodes of alternating polarity [Fig. 1(a)]. This structure constitutes two back-to-back connected Schottky barriers. Since the electric field collecting the photocarriers, created by an interdigitated capacitor as in Fig. 1(a), decays exponentially away from the surface, this structure makes it possible to perform surface-sensitive photocapacitance measurements.

Unlike in conventional photocapacitance experiments with widely separated contacts, the interdigitated capacitor has a measurable capacitance even in the absence of any carriers. The interdigitated capacitor on Fig. 1(a) has a dark capacitance of 25 pF at 4 K. Under illumination, the photocarriers are spatially separated by the electric field of the interdigital electrodes, creating space-charge regions. The capacitance of the space-charge regions is parallel with the capacitance between the interdigital electrodes, resulting in an increase in total capacitance of the chip under illumination.

The periodic electrode pattern was fabricated by standard chlorobenzene lift-off contact photolithography, using Al metallization. The samples were packaged in rectangular six-pin packages, obtained from SAWTEK, and cooled down in an optical helium gas flow cryostat. A 250-W tungsten halogen lamp and either a prism or grating monochromator were used to illuminate the chip. A low-pass filter blocking all light with wavelengths shorter than 0.6 μm was used together with the grating monochromator to intercept harmonics. All measured spectra were normalized for the output of the halogen lamp, taking the output at 0.85 μm as reference.

The samples used for this study were undoped semi-insulating GaAs grown by the liquid encapsulated Czochralski (LEC) technique.

III. RESULTS

Typical photocapacitance spectra measured at 13 K are shown in Figs. 2(a) and 2(b). Below the band gap of GaAs at $E_g = 1.52$ eV, the spectrum produces that previously reported for $EL2$ in semi-insulating GaAs.[10] The 1-MHz photoconductance and photocapacitance spectra were identical. The spectra could be extended to above-band-gap illumination.

Contrary to all expectations, even in the above-band-gap range the spectra are due almost entirely to $EL2$ and not to band-to-band transitions, as evidenced by the ob-

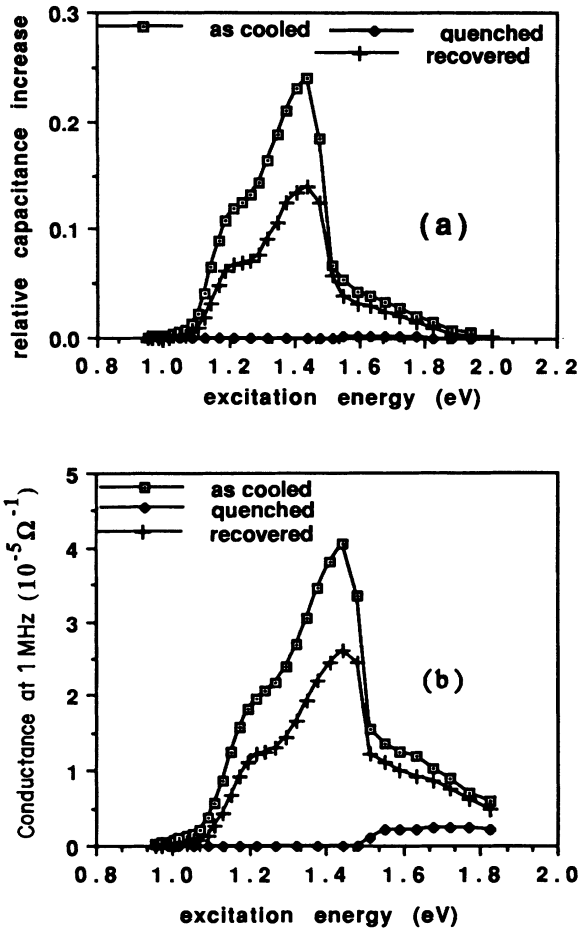

FIG. 2. (a) The photocapacitance and (b) the photoconductance spectra of $EL2$ in LEC surface ionization (SI) GaAs at 13 K, full spectral width 0.015 μm. The spectra shown are from the sample cooled in the dark, quenched by 1-μm illumination and subsequently optically recovered by 0.7-μm light.

servation that they are almost fully quenched by 1-μm illumination when $EL2$ is transferred into the metastable state. They are thermally recovered, like $EL2$, by annealing near 120 K. A very small band-to-band contribution may be due to the fact that electron-hole pairs created by direct band-to-band excitation are subject to fast recombination, whereas recapture of electrons by $EL2^+$ is hindered by a capture barrier of 0.07 eV (Ref. 11) (the lack of persistent photoconductivity at 4 K might be due to parallel athermal capture mechanisms). This would result in a very long lifetime of photoelectrons ionized from $EL2$, by far exceeding that of electron-hole pairs.

In contrast to the low-temperature observations, only intrinsic photocapacitance can be observed at room temperature (Fig. 3). Note the second threshold at 1.82 eV (reported here), that can be ascribed to scattering of hot photoelectrons in the Γ valley to the indirect L minimum of the conduction band, where their recombination has to be phonon assisted, resulting in longer lifetime. From this model, the threshold is above the energy gap by $(E_L-E_\Gamma)(m_e^*+m_h^*)/m_h^*$, in good agreement with the

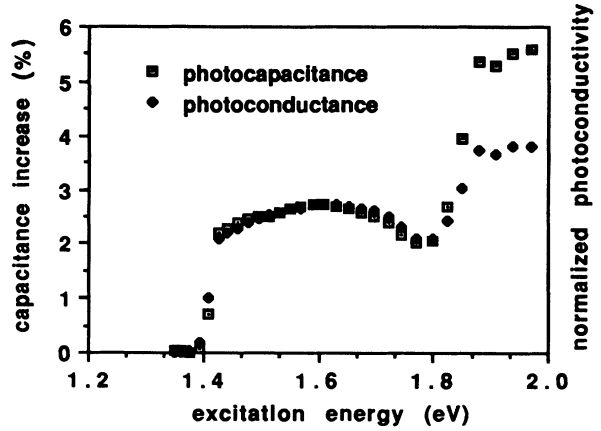

FIG. 3. The photcapacitance (curve 1) and rf photoconductance (curve 2) spectra of LEC SI GaAs at $T=290$ K, measured with the grating monochromator with a spectral resolution of 0.01 μm.

observed value of 0.4 eV. The factor $[(p^2/m_e^*)+(p^2m_h^*)]/(p^2/m_e^*)=(m_e^*+m_h^*)/m_h^*$ is the ratio of the sum of the kinetic energies of the photoelectron and the photohole to the kinetic energies of the photoelectron only.

Another dramatic manifestation of the photoelectron lifetime effect is the *reduction* by about an order of magnitude of $EL2$-related photoconductivity at 4 K, excited by below-band-gap light when the sample is simultaneously illuminated with above-band-gap light, such as a 1-mW He-Ne laser (Fig.4). The magnitude of this reduc-

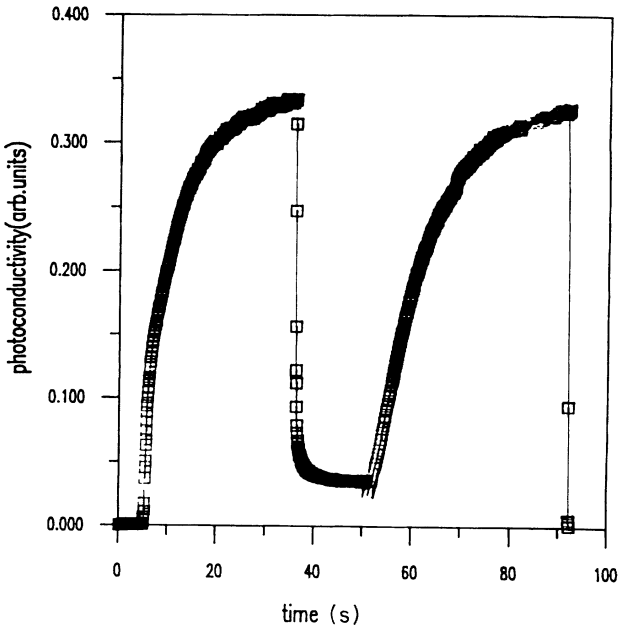

FIG. 4. The dc photoconductance transients at 4 K, illustrating the two beam effects. From $t=12$ to 37 s, the $EL2$ is illuminated with 0.85-μm light. At $t=37$ s, the 1-mW He-Ne laser was also turned on, at $t=51$ s the He-Ne laser was turned off, and at $t=91$ s the 0.85-μm illumination was turned off.

tion increases with the ratio of intensities of the laser light to that of the below-band-gap light. This phenomenon can be understood in terms of the reduction of photoelectron lifetime caused by holes created by the laser light. In the absence of holes, the photoelectron lifetime is determined by the very slow recombination process $EL2^{+}+e^{-} \Longrightarrow EL2^{0}$. However, once the laser illumination creates holes with a rate exceeding the rate of electron recombination with $EL2^{+}$, the photoelectron lifetime is determined by the electron-hole recombination rate rather than by the rate of electron capture by $EL2^{+}$. The resulting decrease in photoelectron lifetime is the most likely cause of the observed decrease in $EL2$-related extrinsic photoconductance upon simultaneous He-Ne laser illumination.

The most important result is the observation that recovery of the $EL2$ spectra, as well as the quenching of it, is obtained at 4 K, depending upon the photon energy of the illuminating light. In Fig. 2, the $EL2$-related photoconductance and photocapacitance spectra are shown after the $EL2$ is quenched by 1-μm light and subsequently recovered with 0.7-μm light. After full photoquenching of the $EL2$, the original photocapacitance spectrum can easily be recovered. The ratio of photocapacitance after full quenching, and subsequent optical recovery of the $EL2$ to photocapacitance of the sample cooled in the dark, can be as much as 0.6. If the sample at 4 K is illuminated by either white light or through a prism monochromator with fully opened aperture, so that both $EL2$ quenching and recovering illumination are transmitted, a steady value of the photocapacitance is established, which is determined by the intensity ratio of recovering to quenching light.

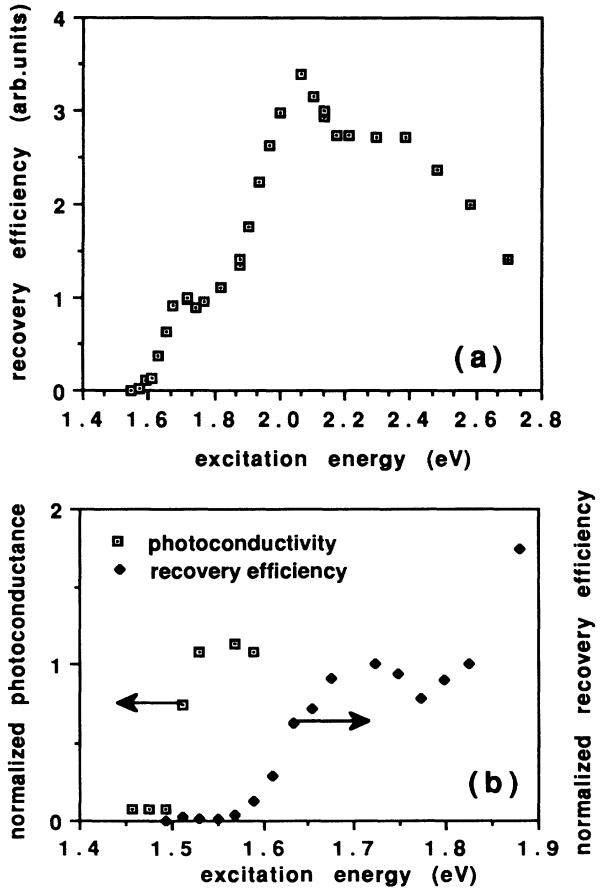

FIG. 5. $EL2$ optical recovery efficiency spectrum at 4 K. (a) Full spectrum 0.03-μm full spectral width. (b) Onset of the optical recovery (0.01-μm spectral width) compared with the onset of band-to-band transitions seen from photoconductance after $EL2$ photoquenching. The normalized photoconductance spectrum at 4 K after $EL2$ was photoquenched, is also given to show the energy of the band gap.

The spectral dependance of the $EL2$ optical recovery efficiency (Fig. 5) was measured as a difference between 0.85-μm photoconductance (or photocapacitance) before and after 2-min exposure to monochromatic recovering light. Photoconductance was fully quenched after each data point. Since only a small fraction of $EL2$ was recovered after 2-min illumination with recovering light, the change in photoconductance is proportional to the initial slope of the recovery transient and thus to the recovery efficiency. At the peak of the photorecovery spectrum at $h\nu=2.1$ eV, the efficiency of optical recovery is three times that of photoquenching at $h\nu=1.2$ eV, both efficiencies taken as fractions of recovered (quenched) $EL2$-related photoconductance and photocapacitance per minute of illumination, normalized for the output of the 250-W halogen lamp. These results should be compared with the observation of the 100% optical recovery at 4 K of the $EL2$-related 0.65-eV photoluminescence band by 2.41-eV light from an argon laser,[12] although the photorecovery was three orders of magnitude slower than the photoquenching.

IV. DISCUSSION

The main question to be addressed in this section is the mechanism of the observed optical recovery of the $EL2$ by above-band-gap illumination. There are two possibilities to consider. The first is that the optical recovery is due to an internal transition of the $EL2^{*}$. This possibility can be ruled out, since a spectrum due to an internal transition should be expected to be of the symmetric Gaussian shape and much narrower than actually observed. On the contrary, the observed optical recovery spectrum (Fig. 5) is extremely wide and asymmetric, with a pronounced low-energy threshold. The second possibility is that the return of the $EL2$ from the metastable to the ground state is driven by energy released by electron-hole recombination. The evidence in favor of this mechanism comes mainly from the similarity of the spectrum of the optical recovery of the $EL2$ at 4 K (Fig. 5) to the intrinsic photoconductance and photocapacitance spectra at 290 K, the latter being entirely due to the electron-hole-pair conductivity (Fig. 3). This mechanism is widely known as the recombination-enhanced defect reaction mechanism. It requires the presence of a defect level capable of trapping electrons or holes. Since the threshold of the optical recovery at 1.6 eV is above the band edge of GaAs at 4 K ($E_g=1.52$ eV), the carrier trap level responsible for the optical recovery should be outside the band

gap (Fig.6). The logical candidate for the carrier trap is the acceptor state of the metastable state, $(EL2^*)^{-/0}$. The energy level of the acceptor state $(EL2^*)^{-/0}$ was extrapolated from the pressure-dependent measurements by Baj and Dreszer[6] to be just above the bottom of the conduction band of GaAs at the ambient pressure [Fig. 6(a)].

This model also provides a consistent explanation for a very weak (two to three orders of magnitude less efficient than the photoquenching) recovery by $h\nu < E_g$ light, which was observed by some authors,[3,4] but not by others.[2] Indeed, a hot electron-hole pair will result in recombination-induced $EL2^* \Rightarrow EL2^0$ conversion, even if created by extrinsic illumination via a partially filled level in the energy gap such as $(EL2)^{0/+}$, although this two-step process is far less efficient than one-step recovery by intrinsic light [Fig. 6(b)]. According to this model, since GaAs samples with greater concentration of compensating acceptors contain more $EL2^+$ and therefore allow more efficient hole creation, they should exhibit more efficient optical recovery. In agreement with this conclusion, the optical recovery of $EL2$ by below-band-gap illumination was found to be most efficient[13,14] in GaAs grown by molecular-beam epitaxy (MBE) at temperatures around 200 °C, in which the concentration of $EL2^+$ is of the order of $10^{18}/\text{cm}^3$ [more than two orders of magnitude greater than in the bulk LEC grown GaAs (Ref. 15)].

From the temperature and pressure dependencies of carrier concentration from pressures above 0.3 GPa, Baj and Dreszer[6] extrapolated that the $(EL2^*)^{-/0}$ level should be higher than the bottom of the conduction band

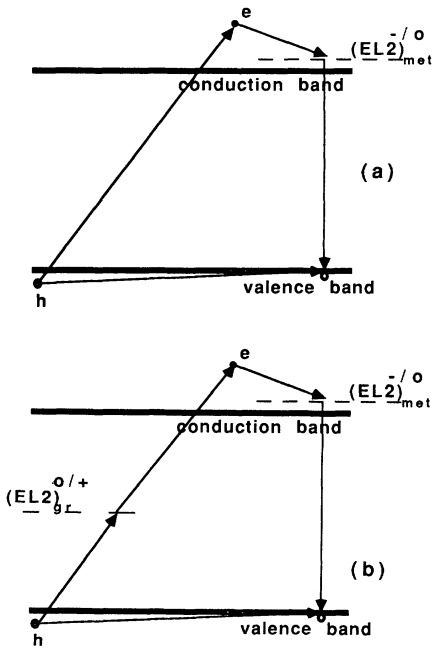

FIG. 6. Electron-hole recombination-induced mechanism of the optical recovery of the $EL2$ (schematic). (a) Highly efficient recovery of the $EL2$ by above-band-gap illumination, discovered in this work. (b) Very low efficiency sample-dependent recovery of the $EL2$ by below-band-gap illumination via the $(EL2)^{0/+}$ defect level.

at ambient pressure by $E_T = 16$ meV. From the optical recovery spectrum with the onset approximately at $E_{\text{rec}} = 1.6$ eV, the minimum kinetic energy that the hot photoelectron must have to be captured by $(EL2^*)^{-/0}$ can be obtained as $E_c = (E_{\text{rec}} - E_g)m_h^*/(m_e^* + m_h^*) = 0.07$ eV. The difference $E_{em} = E_c - E_T \approx 0.05$ eV gives the value of the emission barrier in a configuration coordinate model of $(EL2^*)^{-/0}$. The presence of the emission barrier explains the long lifetime of an electron on $(EL2^*)^{-/0}$ needed for the hole capture, resulting in an efficient optical recovery. The large difference between the capture barrier of 0.07 eV and the thermal height of 0.016 eV of the resonant acceptor level is indicative for lattice relaxation upon electron capture into the acceptor level of $EL2^*$.

In conclusion, the technique presented here made possible direct observation of the optical recovery of $EL2$ in semi-insulating GaAs at ambient pressure by intrinsic illumination at 4 K. It opens the door for optical characterization of defects with levels in the conduction and valence bands.

ACKNOWLEDGMENTS

The authors want to thank Piotr Dreszer and Professor P. Y. Yu for helpful discussions and J. Wheelan, D. Kuchta, and Xin Wu for expert advice on photolithography, Dr. W. Ford of Harris Microwave for the semi-insulating GaAs, and Dr. Robert Kindall of SAWTEK, Inc. for providing the packages. Photolithography was done in the Microfabrication Laboratory, EECS Department. The help of Microlab's staff is acknowledged. This work was supported by the Director, Office of Energy Research, Office of Basic Energy Sciences, Materials Science Division of the U.S. Department of Energy under Contract No. BE-AC03-76SF00098. One of us acknowledges partial support from the AT&T Foundation.

APPENDIX: THE ELECTROSTATIC POTENTIAL OF A PERIODIC GRATING OF INTERDIGITAL ELECTRODES OF ALTERNATING POLARITY

Let us calculate the Coulomb potential created by an infinite periodic array of electrodes of alternating polarity of infinite length and the width of a quarter period. In a general representation, the electrostatic potential can be expressed as a convolution,

$$\phi(\mathbf{r}) = (1/4\pi\epsilon_0\epsilon)\int \rho(\mathbf{r}')/|\mathbf{r}-\mathbf{r}'|d^3\mathbf{r}' \qquad \text{(A1)}$$

where ϵ is dielectric constant,

$$\rho(x,y,z) = \rho(x)\delta(z)$$

is the charge distribution, $\delta(z)$ is the Dirac delta function (z is the direction of surface normal),

$$\rho(x) = \sigma \quad \text{if } -\lambda/8 + \lambda n < x < \lambda/8 + \lambda n \ ,$$

n is any interger,

$$\rho(x)=-\sigma \quad \text{if } -\lambda/8+\lambda n+\lambda/2<x<\lambda/8+\lambda n+\lambda/2 ,$$
$$\rho(x)=0 \quad \text{elsewhere} , \tag{A2}$$

where σ is a charge of an electrode divided by its width [Fig. 1(b)].

The convolution (A1) can be calculated through the Fourier transforms

$$\phi(\mathbf{k})=\int \phi(\mathbf{r})\exp(i\mathbf{k}\cdot\mathbf{r})d^3r$$
$$=(1/\epsilon_0\epsilon)\int \rho(\mathbf{r})\exp(i\mathbf{k}\cdot\mathbf{r})d^3r$$
$$\times\int 1/(4\pi r')\exp(-i\mathbf{k}\cdot\mathbf{r}')d^3r' . \tag{A3}$$

From a well-known equation

$$\int 1/(4\pi r')\exp(-i\mathbf{k}\cdot\mathbf{r}')d^3\mathbf{r}'=1/k^2 . \tag{A4}$$

The Fourier transform of $\rho(\mathbf{r})$ can be rewritten as

$$\rho(\mathbf{k})=\int_{-\lambda/8}^{\lambda/8}\rho(x)\exp(ik_x x)dx$$
$$\times\left[1-2\sum_{m=1}^{N}\cos(m+\tfrac{1}{2})k_x\lambda\right.$$
$$\left.+2\sum_{m=1}^{N}\cos(mk_x\lambda)\right]\delta(k_y) , \tag{A5}$$

where $2N$ is the number of electrodes of each sign (assumed to be very large). $\rho(\mathbf{k})$ does not depend on k_z. The expression in square brackets is essentially not zero only if

$$k_x=2\pi(2n+1)/\lambda . \tag{A6}$$

Taking (A2) into account, one can rewrite (A5) for these values of k_x as

$$\rho(2\pi(2n+1)/\lambda,k_y,k_z)=\lambda\sigma\sin[\pi(2n+1)/4](4N+1)$$
$$\times[\pi(2n+1)]^{-1}\delta(k_y) . \tag{A7}$$

Substituting (A7) and (A4) into (A3), using (A6), and taking the inverse Fourier transform, one obtains

$$\phi(\mathbf{r})=[\lambda\sigma(4N+1)/\epsilon_0\epsilon]\sum\exp[i2\pi(2n+1)x/\lambda]\sin[\pi(2n+1)/4][\pi(2n+1)]^{-1}$$
$$\times\int_{-\infty}^{\infty}\{k_z^2+[2\pi(2n+1)/\lambda]^2\}^{-1}\exp(ik_z z)dk_z/(2\pi) . \tag{A8}$$

The integral can easily be calculated by replacing the contour of integration along the real axis with the infinite semicircle in the upper half plane of the complex variable plane and the infinitesimal circle around the pole $k_z=2\pi i(2n+1)/\lambda$. The result is

$$\int_{-\infty}^{\infty}\{k_z^2+[2\pi(2n+1)/\lambda]^2\}^{-1}\exp(ik_z z)dk_z/(2\pi)$$
$$=\{\lambda\exp[-2\pi(2n+1)z/\lambda]\}\{[4\pi(2n+1)]\}^{-1} . \tag{A9}$$

Substituting (A9) into (A8), we obtain the expression for the Coulombic potential as a series of decaying exponentials

$$\phi(\mathbf{r})=[\lambda^2\sigma(4N+1)/\epsilon_0\epsilon]$$
$$\times\sum_{n=0}^{\infty}\exp[i2\pi(2n+1)x/\lambda]$$
$$\times\exp[-2\pi(2n+1)z/\lambda]$$
$$\times\sin[\pi(2n+1)/4]\{[2\pi(2n+1)]\}^{-2} . \tag{A10}$$

For the depth $z\gg\lambda/6\pi$, the series is dominated by the first term and then (A10) can be approximated as

$$\phi(r)\approx[\lambda^2 s(4N+1)/4\pi\sqrt{2}\epsilon_0\epsilon]$$
$$\times\exp(i2\pi x/\lambda)\exp(-2\pi z/\lambda) , \tag{A11}$$

i.e., an exponentially decaying potential with a penetration depth of $\lambda/2\pi$.

[1]G. M. Martin and S. Makram-Ebeid, in *Deep Centers in Semiconductors,* edited by S. T. Pantelides (Gordon and Breach, New York, 1985).

[2]J. C. Parker and R. Bray, Phys. Rev. B **37**, 6368 (1988).

[3]M. Tajima, H. Saito, T. Iino, and K. Ishida, Jpn. J. Appl. Phys. **27**, L101 (1988).

[4]D. W. Fischer and M. O. Manasreh, Appl. Phys. Lett. **54**, 2018 (1989).

[5]M. Baj and P. Dreszer, Phys. Rev. B **39**, 10 470 (1989).

[6]M. Baj, P. Dreszer, and A. Babinski, Phys. Rev. B **43**, 2070 (1991).

[7]P. Dreszer, M. Baj, and K. Korzeniewski, Mater. Sci. Forum **83-87**, 875 (1992).

[8]T. Sugiyama, K. Tanimura, and N. Itoh, Appl. Phys. Lett. **55**, 639 (1989).

[9]M. D. Sturge, Phys. Rev. **127**, 768 (1962).

[10]P. Trautman and J. P. Walczak, in *Semi-Insulating III-V Materials,* edited by G. Grossmann and L. Ledebo (Hilger, Bristol, 1988), p. 375.

[11]M. Kaminska *et al.*, Appl. Phys. Lett. **43**, 302 (1983).

[12]M. Tajima, Jpn. J. Appl. Phys. **23**, L690 (1984).
[13]A. Kurpiewski, M. Palczewska, M. Kaminska, and E. R. Weber, Acta Phys. Pol. (to be published).
[14]K. Khachaturyan, E. R. Weber, and R. M. White, Phys. Rev. B **45**, 4258 (1992).
[15]M. Kaminska, Z. Liliental-Weber, E. R. Weber, T. George, J. B. Kortright, F. W. Smith, B.-Y. Tsaur, and A. R. Calawa, Appl. Phys. Lett. **54**, 1881 (1989).